NASA/TM-1998-208452

Parameter Estimation of Actuators for Benchmark Active Control Technology (BACT) Wind Tunnel Model With Analysis of Wear and Aerodynamic Loading Effects

Martin R. Waszak and Jimmy Fung
Langley Research Center, Hampton, Virginia

National Aeronautics and
Space Administration

Langley Research Center
Hampton, Virginia 23681-2199

July 1998

Acknowledgments

Available from the following:

NASA Center for AeroSpace Information (CASI)
7121 Standard Drive
Hanover, MD 21076-1320
(301) 621-0390

National Technical Information Service (NTIS)
5285 Port Royal Road
Springfield, VA 22161-2171
(703) 487-4650

Contents

Tables

Figures

Symbols

BACT   Benchmark Active Control Technology

c_m arbitrary weighting on frequency response magnitude error

c_p arbitrary weighting on frequency response phase error

e   frequency response error vector

FFT   Fast Fourier Transform

J cost function

$K_{\Delta hp}$ gain on differential hydraulic pressure

K_ε gain on control surface position error

k actuator transfer function gain

LS   lower spoiler

M Mach number

mag   magnitude

Δmag   frequency response magnitude error

PAPA   Pitch and Plunge Apparatus

p first-order actuator pole

phs   phase

Δphs   response phase error

q dynamic pressure

S   diagonal weighting matrix

s Laplace variable

TDT   Langley Transonic Dynamics Tunnel

TE   trailing edge

US   upper spoiler

y   vector of frequency response magnitude and phase

$\dfrac{\Delta\theta}{\hat{\theta}}$ normalized parameter estimate error

Δhp   differential hydraulic pressure

δ control surface position

δ_c commanded control surface position

ε^2 weighted mean squared frequency response error

ε^2_{min} minimal allowable weighted mean squared frequency response error

ζ second-order actuator damping ratio

ω second-order actuator frequency

Subscripts:

a   from analysis or estimation

e   from experiment

i   vector index

init   initial quess

new   updated estimate

opt   optimal estimate

Abstract

This report describes the development of transfer function models for the trailing-edge and upper and lower spoiler actuators of the Benchmark Active Control Technology (BACT) wind tunnel model for application to control system analysis and design. A simple nonlinear least-squares parameter estimation approach is applied to determine transfer function parameters from frequency response data. Unconstrained quasi-Newton minimization of weighted frequency response error was employed to estimate the transfer function parameters. An analysis of the behavior of the actuators over time to assess the effects of wear and aerodynamic load by using the transfer function models is also presented. The frequency responses indicate consistent actuator behavior throughout the wind tunnel test and only slight degradation in effectiveness due to aerodynamic hinge loading. The resulting actuator models have been used in design, analysis, and simulation of controllers for the BACT to successfully suppress flutter over a wide range of conditions.

Introduction

The ability of an active control system to accomplish the function for which it was designed depends to a large degree on the accuracy of the mathematical models used to describe the dynamic behavior of the physical system to be controlled. A crucial element of the overall system is the actuator. The commanded control inputs need to be accurately produced by the actuators in order to achieve the desired level of performance. Mathematical models that characterize the dynamic response of the actuators are therefore key requirements for design, analysis, and simulation of any control system.

The objective of this investigation is to develop a set of actuator models for the Benchmark Active Control Technology (BACT) wind tunnel model (refs. 1 and 2) that is appropriate for application to control system analysis and design. Although this type of application does not require the actuator model structure and parameter estimates to be particularly accurate, the dynamic input-output properties of the actuators over the frequency range of interest for the BACT wind tunnel model should be fairly accurate.

Control system design usually takes into account design model variations and uncertainty in the form of gain and phase margins. Typical gain and phase margins might be ±6 dB and ±30°, respectively. Errors in the actuator models should only represent a small fraction of these margins—perhaps 10 percent or so. In this report, input-output frequency response accuracy, measured in terms of magnitude and phase compared with experimental frequency response data, is the basis for the acceptability of the actuator model structure and parameter estimates. The accuracy of the parameter estimates themselves, however, is not considered.

Development of the actuator models begins by an assessment of the physical systems of the BACT wind tunnel model and a review of the available data. An actuator model structure is then chosen based on the physical characteristics of hydraulic actuation systems. A simple parameter estimation procedure based on minimizing weighted frequency response error in a quasi-Newton scheme is outlined. The parameters of the model structure are determined from experimental frequency response data and analyzed to assess variations in the dynamic input-output characteristics of the actuators over time (due to servo loop gain variations and bearing, seal, and sensor wear) and the effects of control surface hinge loading due to aerodynamics.

Note that frequency response data are treated as the truth data for the parameter estimation process. The frequency response data are based, however, on *estimates* of the power spectra of actuator responses obtained from experimental data with fast Fourier transform (FFT) techniques. As a result, the frequency response data have associated estimation errors that depend on the way in which the time histories were recorded and the manner in which the FFTs were computed. (See ref. 3.) The errors introduced by the FFT process are not considered herein.

Part of the information presented in this report was included in a paper entitled "Parameter Estimation and Analysis of Actuators for the BACT Wind-Tunnel Model" that was presented at the AIAA Atmospheric Flight Mechanics Conference, San Diego, California, July 29–31, 1996, and is available as AIAA-96-3362.

Experimental Setup

The Benchmark Active Control Technology (BACT) project is part of the Benchmark Models Program (ref. 4) for studying transonic aeroelastic phenomena. The BACT system was developed to collect high quality unsteady aerodynamic data (pressures and loads) near transonic flutter conditions and to demonstrate active flutter suppression. The BACT system consists of a rigid wing section and a flexible mounting system. (See refs. 5 and 6.) Figure 1 is a photograph of the BACT wing section and the flexible mount.

The wind tunnel model is a rigid rectangular wing with an NACA 0012 airfoil section and is equipped with a trailing-edge control surface and upper and lower surface spoilers that are controlled independently by hydraulic actuators. It is instrumented with pressure transducers, accelerometers, control surface position sensors, and hydraulic pressure transducers. Figure 2 is a photograph of the wing section showing

dimensions of the various components including the control surfaces.

The wing is mounted to a device called the Pitch and Plunge Apparatus (or PAPA) which is designed to permit motion in principally two modes—rotation (or pitch) and vertical translation (or plunge). The BACT system was tuned to flutter within the operating range of the Langley Transonic Dynamics Tunnel (TDT) (ref. 7) in which the system was tested. During operation the mounting system is isolated from the wing section by a splitter plate. In addition, the mounting system is isolated from the airflow by a faring that is secured to the splitter plate and the wall of the test section. Figure 3 depicts a diagram of the wind tunnel test section showing how the BACT system was mounted in the wind tunnel.

The actuators in the trailing edge and upper and lower spoiler control surface assemblies were specifically designed for the BACT wind tunnel model because of the space limitations arising from placing the two spoilers and the trailing-edge control surface in close proximity. The trailing-edge control surface is driven by a rotary vane actuator and the spoilers are driven by piston actuators. (See ref. 8.) Each actuator has a servo loop as depicted in the block diagram in figure 4. The control surface position sensors and hydraulic pressure transducers were used as servo feedback signals. The gains on position error K_ε and
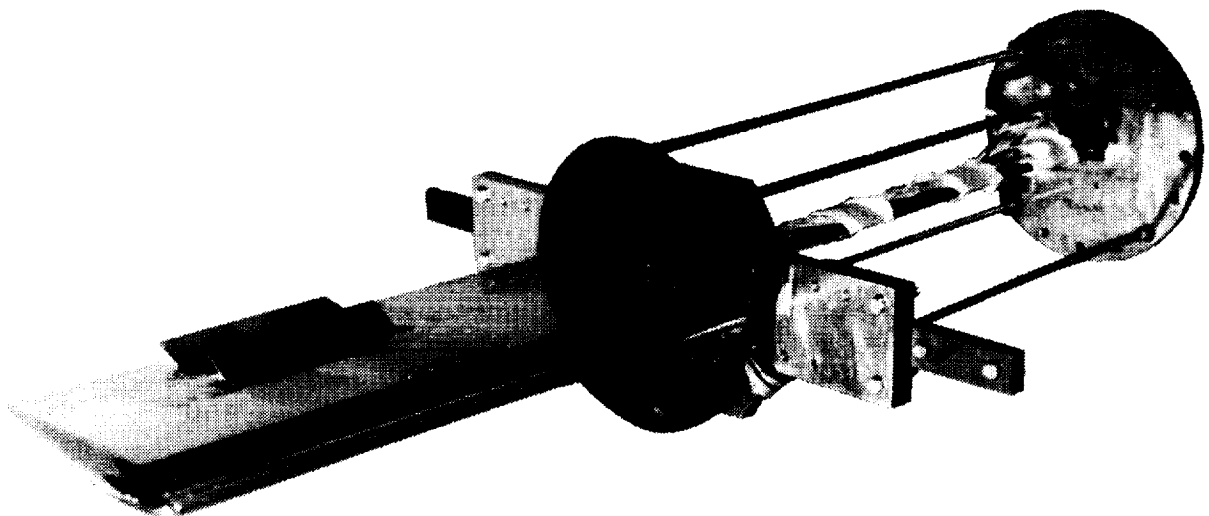

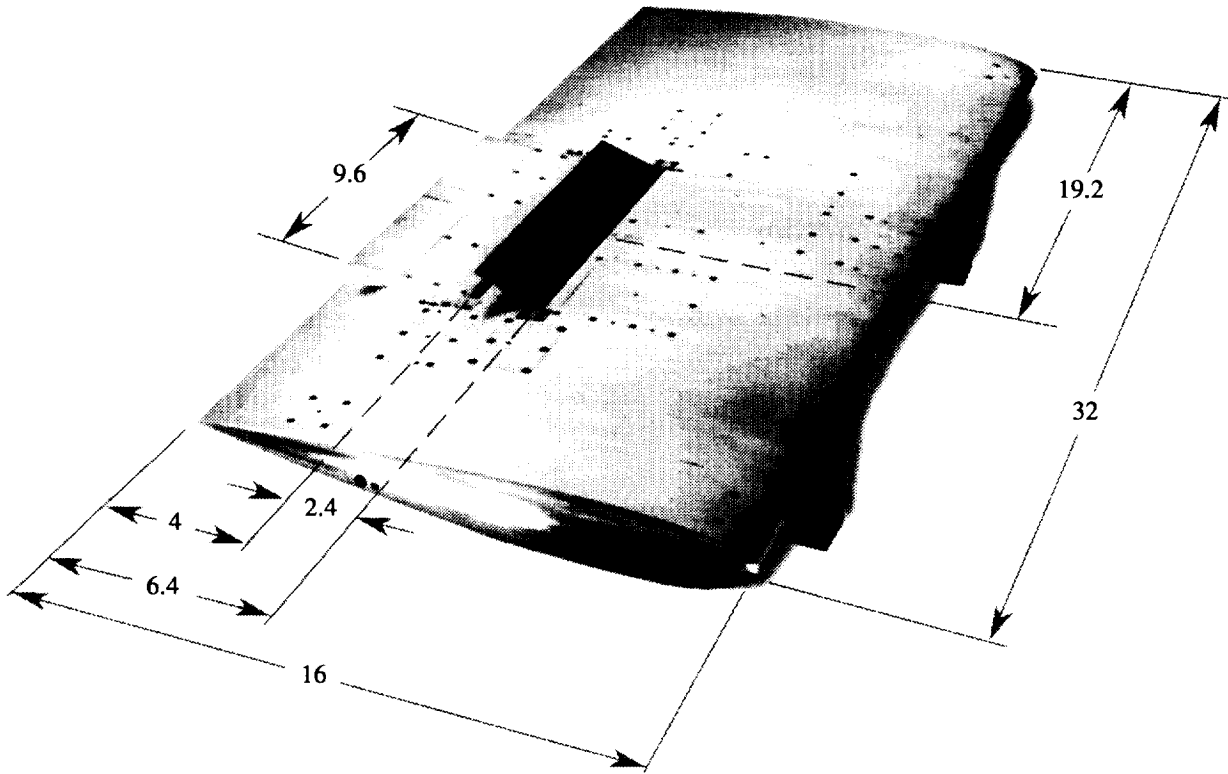Figure 1. BACT wing section and flexible mount.

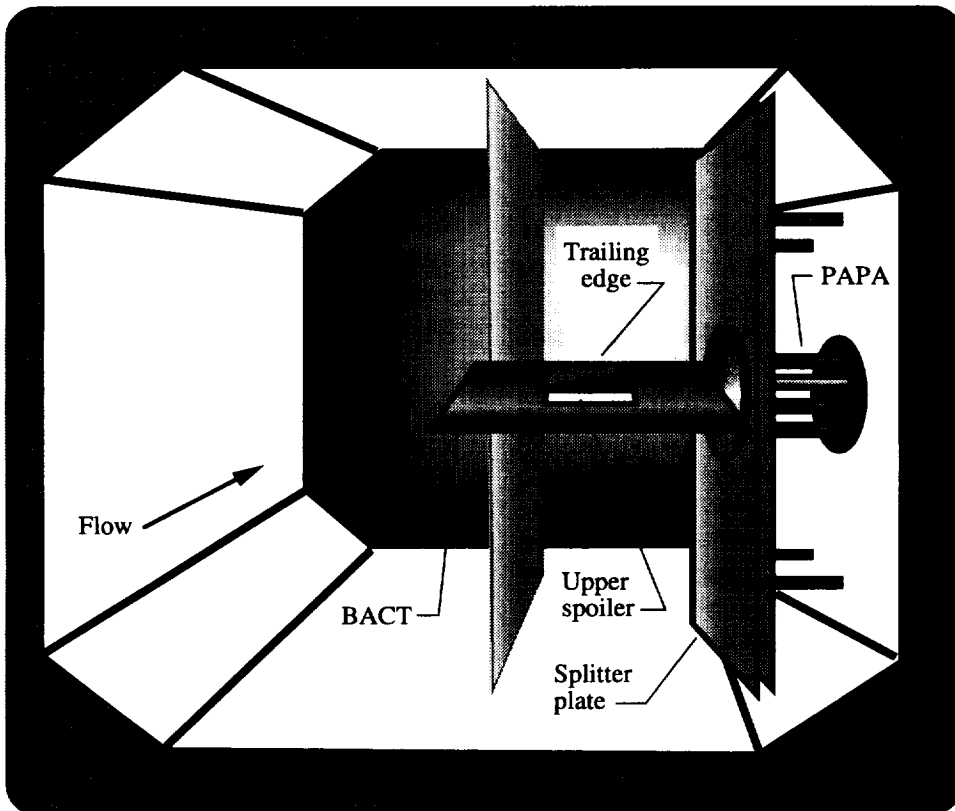Figure 2. BACT wind tunnel model. Dimensions are in inches.

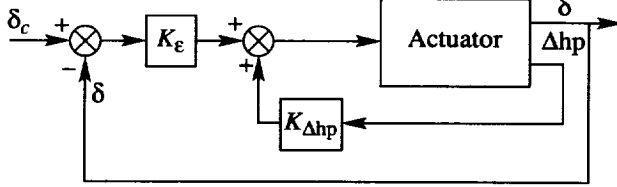Figure 3. BACT wind tunnel test arrangement.

3

Figure 4. Servo loop for BACT actuators.

differential hydraulic pressure $K_{\Delta hp}$ could be adjusted to alter the response characteristics of the actuator.

Experimental Data

A large set of experimental frequency response data for the BACT actuators was available from calibration and wind tunnel tests. The data were not generated with parameter estimation in mind and consequently were not ideal for parameter estimation applications. However, the data provide a basis upon which actuator models with sufficient accuracy for control system design applications can be obtained.

The actuator data were collected during an experiment that took place early in 1995. The test lasted approximately 4 weeks during which over 2300 test points were recorded. The average duration of each test point was about 5 minutes. About half the test points involved some level of actuator activity. Roughly three-quarters of the test points involving control activity used the trailing-edge control and the other quarter used the upper spoiler. The lower spoiler was used very little during the test.

Excitation of the control surfaces for actuator performance assessments was performed periodically throughout the test at a variety of Mach numbers and dynamic pressures. The excitations were performed under open-loop conditions; that is, there was no feedback around the BACT system. Commanded excitations, either linear sine sweeps or random sequences, had a duration of either 25 or 75 seconds. Control surface commands and the resulting control surface position signals were recorded at a rate of 200 samples per second.

The time response data were converted into frequency response form. Fast Fourier transform (FFT) techniques were used to compute estimates of the cross- and auto-spectral density of actuator command

and control surface position. The frequency response of the actuator was then determined by taking the ratio of the appropriate cross- and auto-spectra. The FFTs were computed by the method described in reference 9 and by using a Hanning window, 2K data blocks, and 75 percent overlap averaging. These frequency response data are the basis for the actuator modeling that is described subsequently.

As the test progressed, several factors could have influenced the actuator dynamics. Because data were available at various points throughout the test, assessing variations in the actuator dynamic characteristics was possible. The differential hydraulic pressure gain was zero throughout the test but the position error gain of the actuator servo loops was altered at various times during the test to maintain desired response characteristics and to attempt to eliminate chatter that appeared in some control surface responses. The change in the position error gain was not measured nor recorded and thus represents an unknown variation. In addition, the use of the actuators led to wear in the seals, bearings, and position sensor potentiometers that could have altered the actuator responses.

In order to establish a basis for assessment of variations over time, three data sets were chosen to represent data acquired early, in the middle, and late in the test. These data sets are referred to in this report as "Early," "Middle," and "Late," respectively, and roughly correspond to data collected during the first, second, and third weeks of the test. The number of cycles that each actuator completed throughout the test varied considerably. Therefore, the potential for variations over time was different for each actuator.

The effect of aerodynamic loading on the actuator characteristics could also be assessed because data were available at a variety of operating conditions (Mach numbers and dynamic pressures). The experimental data were categorized according to aerodynamic loading conditions, either loaded or unloaded. The loaded condition is therefore representative of a relatively wide range of Mach numbers and dynamic pressures and represents a general basis upon which the effect of control surface hinge loads can be assessed. Comparing frequency responses for the actuator with and without aerodynamic loading gives an indication of the degree to which the actuator behavior could vary over the range of operating conditions.

4

Actuator Model Structure

The mathematical models for the BACT actuators were based on a third-order transfer function structure that characterizes the key features of hydraulic systems (refs. 10 and 11) as shown in the following equation:

$$\frac{\delta(s)}{\delta_c(s)} = \frac{kp\omega^2}{(s+p)(s^2+2\zeta\omega s+\omega^2)} \qquad (1)$$

Here the output δ is the angular position of the control surface and the input δ_c is the actuator command. The four unknown parameters in this transfer function structure are as follows: k is a gain, p is a first-order pole, and ω and ζ are second-order frequency and damping. The first-order pole is associated with the flow of hydraulic fluid through a small orifice and the gain on control surface position error feedback. The second-order frequency and damping are associated with the compressibility of the hydraulic fluid, the inertia of the control surface, the compliance of the structure, and the gain on control surface position error. Note that these parameters are not independent due to coupling via the actuator servo loop. (See fig. 4.)

A transfer function model structure was selected because of its inherently simple structure and the ease with which it can be integrated into control system analysis, design, and simulation. It cannot, however, characterize nonlinearities such as amplitude dependent gains, dead zone and backlash, or position and rate limits. These effects must be addressed by other means and are not addressed here.

Parameter Estimation

The four transfer function parameters from equation (1) were estimated from experimental frequency response data by using the process outlined by the flowchart shown in figure 5. The process involves defining a cost (or error) function and minimizing that function by the selection of the desired parameter set (k,p,ζ,ω). First, an initial parameter set was selected and the resulting analytical frequency response data, in magnitude and phase form, were computed at the same frequencies for which the experimental data were available. The magnitude and phase errors
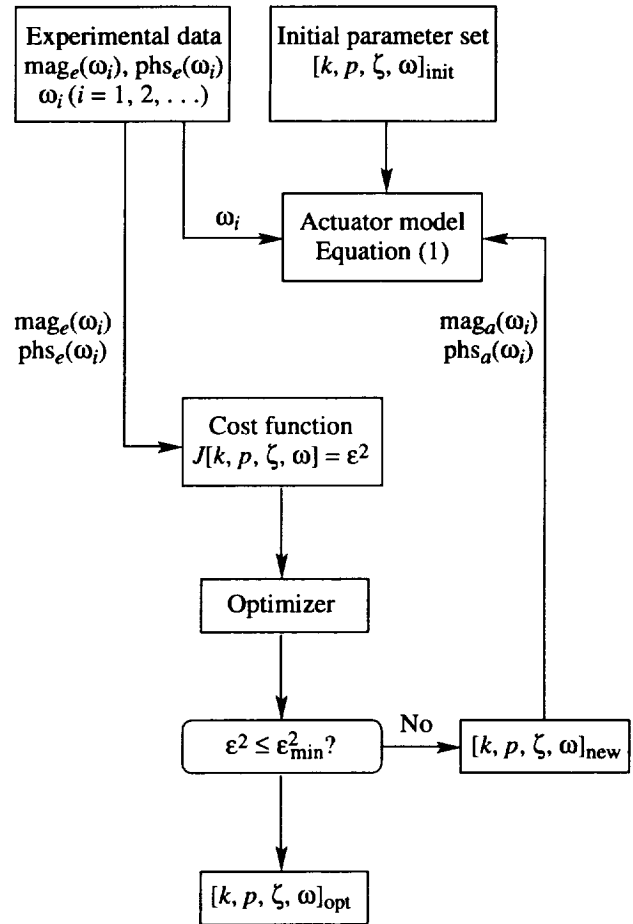

Figure 5. Parameter estimation process.

between the analytical and experimental data were then calculated. A weighted summed square of the transfer function magnitude and phase errors ε^2 was minimized within an optimization routine. The frequency response based on the optimized parameters was then compared with the experimental data to verify the accuracy of the model and the acceptability of the convergence criterion.

The optimizer used a quasi-Newton approach based on the Broyden, Fletcher, Goldfarb, Shanno (BFGS) method for updating the inverse Hessian. (See ref. 12.) MATLAB[1] and the function fminu from the Optimization Toolbox (ref. 13) were used in this study to perform the error minimization. Note, however, that the specific routine is somewhat arbitrary in that any method able to minimize the scalar error function ε^2 could be used.

---

[1]Registered trademark of The MathWorks, Inc.

The convergence criteria for the optimizer were the minimum allowable frequency response error ε^2_{min} and the change in the parameter values between successive iterations $(\Delta\theta/\hat{\theta})_{min}$. These criteria were chosen to achieve qualitatively acceptable approximations to the experimental data and were determined by plotting the experimental frequency response data and the frequency response associated with the estimated transfer function parameters on the same plot. The convergence criteria values were chosen small enough so that the frequency response error was judged to be acceptable but large enough so that convergence could be achieved.

The input-output frequency response error was judged to be acceptable when, in the frequency range from 2 to 10 hertz, the gain differences were less than about 0.1 and phase differences were less than about 3°. These values represent approximately 10 percent of the typical control system gain and phase margins mentioned previously. Errors greater than these were deemed acceptable if they appeared to be due to higher order effects or nonlinearities in the experimental data.

The error function ε^2 was formed in the following manner. The experimental and analytical frequency responses were represented in magnitude and phase form. The magnitude and phase values were stacked to form a vector as shown in the following equation. Each element in the vector corresponds to a particular frequency ω_i at which the experimental data were available.

$$
\mathbf{y} = \begin{bmatrix} mag \\ phs \end{bmatrix} = \begin{bmatrix} mag(\omega_1) \\ mag(\omega_2) \\ mag(\omega_3) \\ \vdots \\ mag(\omega_n) \\ phs(\omega_1) \\ phs(\omega_2) \\ phs(\omega_3) \\ \vdots \\ phs(\omega_n) \end{bmatrix} \quad (2)
$$

An error vector $\mathbf{e}$ was then formed from the difference between the experimental and analytical frequency response data such as

$$
\mathbf{e} = \mathbf{y}_e - \mathbf{y}_a = \begin{bmatrix} mag_e - mag_a \\ phs_e - phs_a \end{bmatrix} = \begin{bmatrix} \Delta mag \\ \Delta phs \end{bmatrix} \quad (3)
$$

where Δmag is the magnitude error and Δphs is the phase error. The weighted summed square error ε^2 was created by the weighted inner product of the error vector with itself and can be written as

$$
\varepsilon^2 = \mathbf{e}^T \mathbf{S} \mathbf{e} \quad (4)
$$

where $\mathbf{S}$ is a diagonal matrix. The diagonal of $\mathbf{S}$ can be written

$$
\begin{aligned}
diag(\mathbf{S}) = [&c_m(\omega_1)\ c_m(\omega_2)\ c_m(\omega_3)...c_m(\omega_n) \\
&c_p(\omega_1)\ c_p(\omega_2)\ c_p(\omega_3)...c_p(\omega_n)] \quad (5)
\end{aligned}
$$

where $c_m(\omega_i)$ and $c_p(\omega_i)$ are arbitrary constants corresponding to the frequency ω_i and n is equal to the number of frequency points in the experimental frequency response data set.

A variety of error weighting schemes were studied to select the diagonal elements of the weighting matrix $\mathbf{S}$. Emphasizing the penalty on phase error over the entire frequency range resulted in acceptable approximation to the experimental data. Several reasons for this result exist. Accurate representation of the phase lag properties of the actuators is more important when applying the actuator models to control system analysis and design because the actuators typically have a much higher bandwidth than the system they control. In addition, magnitude variations in the frequency response data (for example, due to amplitude dependent nonlinearities) played a lesser role in the parameter estimation process by weighting phase error significantly more than magnitude error. Finally, excitation of the actuators was performed over a range of frequencies consistent with the key dynamics of the BACT system and not that of the actuators themselves. The bandwidth of the actuators was about twice the highest excitation frequency. Recall that for a given set of dynamics the effect on the phase response is apparent at a frequency about 1 decade lower than the magnitude response. As a result, for the

available data, there is more information in the phase response than in the magnitude response. For all these reasons, penalizing the phase error more heavily resulted in models that more closely approximate the key dynamics of the actuators.

Application of Parameter Estimation Procedure

The parameter estimation procedure was applied to construct actuator models for the BACT wind tunnel model by using the available experimental frequency response data. The weighting strategy described previously was used with $c_m(\omega_i)$, $i = 1, 2, 3, ..., n$, equal to 1 and the values of $c_p(\omega_i)$, $i = 1, 2, 3, ..., n$, equal to 10. The value for the convergence criteria that resulted in acceptable convergence was $\varepsilon_{min}^2 = 1 \times 10^{-4}$, and $(\Delta\theta/\hat{\theta})_{min} = 1 \times 10^{-4}$, the default values for fminu. In practice, the parameter convergence criterion was active, the minimum error criterion was never satisfied.

The estimation process was initiated with a variety of initial guesses for the unknown parameter set (k, p, ζ, ω). When there was no aerodynamic loading, the initial guess played a relatively small role in convergence. When aerodynamic load was present, however, the solution was more sensitive to the initial parameter set and more iterations were generally required for convergence. The most critical initial parameter values were the first-order pole p and the second-order frequency ω. Several initial guesses were sometimes required to achieve convergence. Ultimately, initial guesses were selected in such a way that parameters for the loaded cases were similar to those for the unloaded cases. These initial guesses also

tended to achieve minima with lower frequency response errors.

Slower convergence for the aerodynamically loaded conditions can be attributed to the nature of the experimental data. Wind tunnel turbulence resulted in lower signal-to-noise ratios and consequently more noise in the frequency response data than when no turbulence was present. Aerodynamic load may also contribute to nonlinearities or higher order effects that cannot be approximated well with the third-order actuator model in equation (1). Nonlinearities, higher order effects, and noise in the experimental frequency response data result in larger weighted summed square frequency response error.

In addition, the sensitivity to the initial guesses for the parameters indicates the possibility of local minima or very flat solution spaces. This problem was addressed by using multiple initial guesses and evaluating the convergence patterns and the similarity of the converged parameter sets. The sensitivity of the converged solutions under load indicates that, although similar accuracy can be achieved over the range of frequencies of interest, the resulting bandwidth and resonant peak properties of the actuators (i.e., the values of p, ω, and ζ) can vary significantly. However, because no experimental data were available near the bandwidth frequencies, the accuracy of the estimates of p, ω, and ζ in terms of bandwidth and resonant peaks could not be addressed in this study.

The estimated parameter sets based on experimental data are shown in tables 1 and 2. (Data were not available for the lower spoiler under load late in the test.) Frequency response data created from the analytical models by using the parameters in tables 1 and 2

Table 1. Analytical Transfer Function Parameters With No Aerodynamic Load

Control surface	Test stage	k, deg/deg	p, 1/sec	ω, rad/sec	ζ
Trailing-edge actuator	Early	1.0198	10 000	165.26	0.5624
	Middle	1.0413	10 000	223.57	0.7269
	Late	1.0159	10 000	212.50	0.5776
Upper spoiler actuator	Early	1.1617	10 000	164.00	0.8478
	Middle	1.1180	10 000	142.02	0.6463
	Late	1.1219	10 000	138.21	0.6024
Lower spoiler actuator	Early	1.0903	10 000	168.45	0.7583
	Middle	1.0362	10 000	155.08	0.6795
	Late	1.0942	10 000	175.77	0.7885

7

Table 2. Analytical Transfer Function Parameters With Aerodynamic Load

Control surface	Test stage	k, deg/deg	p, 1/sec	ω, rad/sec	ζ
Trailing-edge actuator	Early	0.9607	10 000	139.20	0.4281
	Middle	0.9345	10 000	133.44	0.4055
	Late	1.0468	6 898	242.32	0.7475
Upper spoiler actuator	Early	1.1152	9 995	125.65	0.6187
	Middle	1.1702	9 996	135.87	0.6827
	Late	1.0767	2.97×10^8	100.72	0.4615
Lower spoiler actuator	Early	1.0289	9 998	145.07	0.6314
	Middle	1.0265	9 999	150.85	0.6444
	Late	N/A	N/A	N/A	N/A

very closely approximate the experimental data with respect to both magnitude and phase over the frequency range from 0.5 to 12 hertz (at which experimental data were available). Figure 6 shows the frequency responses of the experimental and analytical data for a typical case. Additional plots are presented in the appendix.

Note that the parameters k and p did not vary nearly as much over time and aerodynamic loading condition as did ω and ζ. In addition, the first-order lag p remained very large for both loaded and unloaded conditions throughout the test. As a result,

the term $p/(s + p)$ is almost unity over the range of frequencies of interest for the BACT, and its contribution to the frequency responses based on the transfer function model in equation (1) is negligible. Therefore, the actuator model is in a sense overparameterized and a second-order transfer function of the following form by using the parameter values from tables 1 and 2 could also be used with comparable results:

$$\frac{\delta(s)}{\delta_c(s)} = \frac{k\omega^2}{s^2 + 2\zeta\omega s + \omega^2} \qquad (6)$$

Figure 7 shows the magnitude and phase differences between the frequency responses of the

Model parameters
$k = 1.0767$
$p = 2.97 \times 10^8$ 1/sec
$\omega = 100.72$ rad/sec
$\zeta = 0.46152$
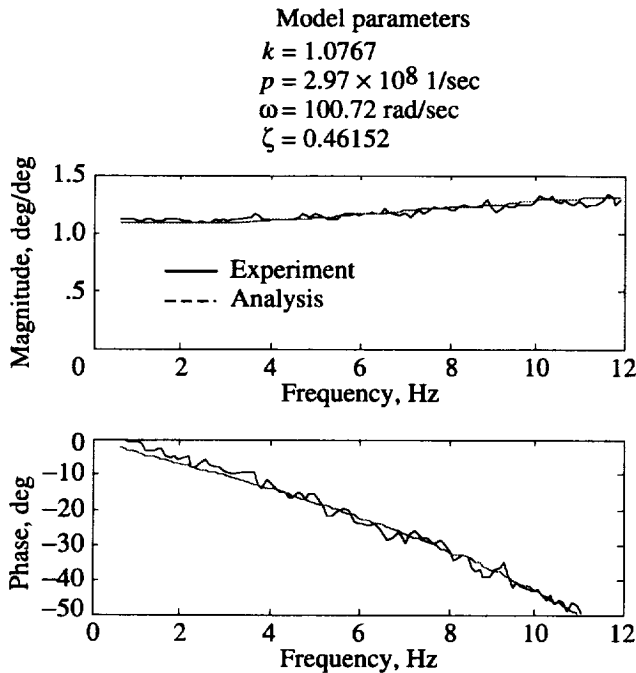
Figure 6. Frequency response for upper spoiler with aerodynamic load. $M = 0.80$; $q = 140$ psf; late in wind tunnel test.
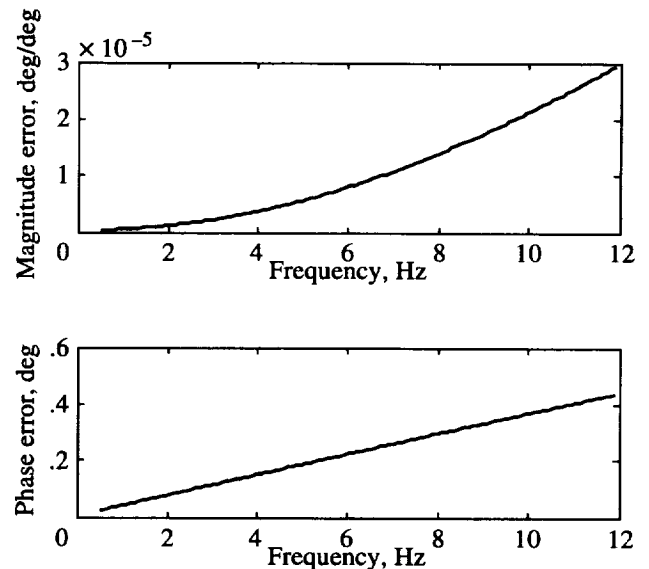

Figure 7. Frequency response error between third- and second-order models of lower spoiler. No aerodynamic load; $M = 0$; $q = 0$ psf; early in wind tunnel test.

8

third- and second-order actuator models, equations (1) and (6), respectively, for a typical case. The parameter values used in each case were identical. The only difference was the omission of p in equation (6). The errors in both magnitude and phase are very small and clearly justify the use of the second-order transfer function form (eq. (6)).

Despite the overparameterization and convergence issues, the parameter estimation process was successful in constructing analytical models of the actuators. Therefore, the actuator models presented in equations (1) and (6) with the parameter values presented in tables 1 and 2 can be effectively utilized to characterize the dynamic behavior of the BACT actuators.

Analysis of BACT Actuator Behavior

With the analytical actuator models obtained during the parameter identification process, an analysis was done to determine consistency of the actuator dynamics during the BACT wind tunnel test. Two issues of primary concern were addressed—the effect of variations over time (i.e., servo gain variations and mechanical wear) and the effect of hinge moments on the dynamic characteristics of the actuators. Variations over time were considered by comparing data over the three test stages (early, middle, and late). Hinge load effects were considered by comparing data for the loaded and unloaded conditions.

If the input-output frequency response behavior of the actuators change significantly over time and/or with hinge loads it would be important to consider these effects in the design of control laws to assure that stability and performance are maintained. Magnitude variations of more that 0.1 and phase variations of more than 3° were deemed unacceptable. These allowable variations correspond to 10 percent of the typical gain and phase margins mentioned previously.

Comparing the data among the three test stages indicate notable differences in the parameters ω and ζ caused by variations over time as can be seen by comparing the data presented in tables 1 and 2. Figures 8 and 9 indicate how actuator frequency and damping parameters varied over time with no aerodynamic hinge load. The effect of the parameter variations is primarily to introduce phase variations in the actuator
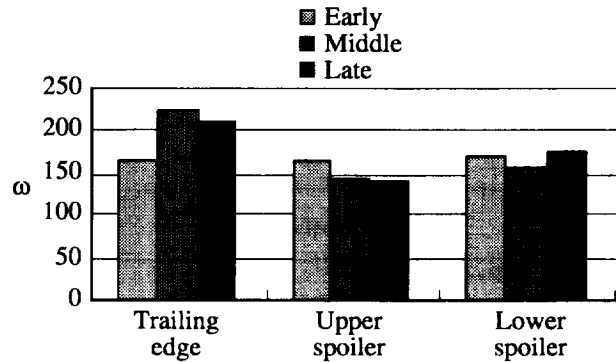
Figure 8. Frequency parameter ω for unloaded conditions throughout wind tunnel test.
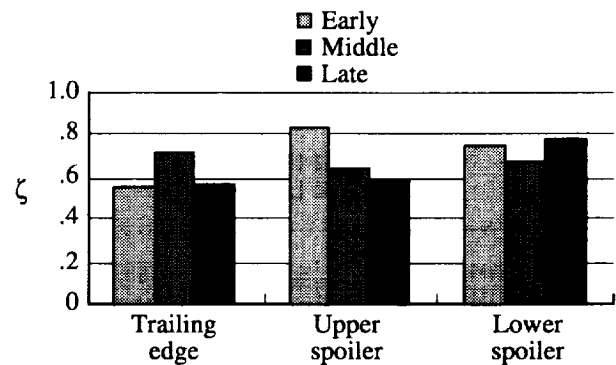

Figure 9. Damping parameter ζ for unloaded conditions throughout wind tunnel test.

frequency response as shown in figure 10, which depicts a chronological comparison of the trailing-edge actuator frequency responses for the unloaded condition ($M = q = 0$) and is representative of the effects of time variations. Additional plots showing the effect of parameter variations are presented in the appendix.

The differences in the phase response over the frequency range from 0.5 to 12 hertz become significant at frequencies beyond 6 hertz. The key aeroelastic frequencies for the BACT wind tunnel model are in the range from 3 to 5 hertz. The smaller variations in phase at these frequencies are generally within the allowable range. However, the variations over time could become significant if phase uncertainty at frequencies beyond 5 hertz was an issue in the control system design. The effect of hinge moment on actuator behavior is less significant. Figures 11 and 12 indicate how actuator frequency and damping parameters varied because of aerodynamic load early in the test.
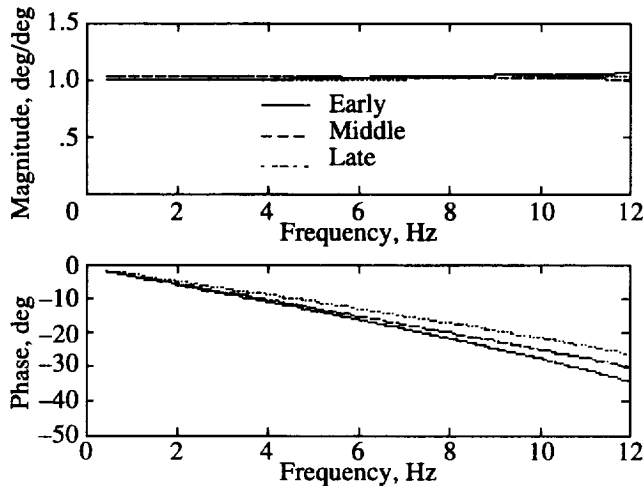
9

Figure 10. Effects of servo gain variations and mechanical wear for trailing-edge actuator frequency response with no aerodynamic load.
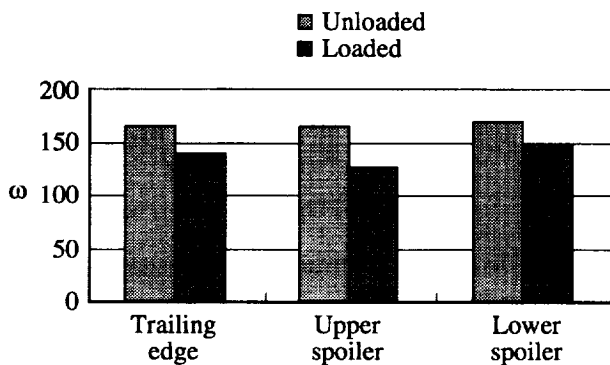

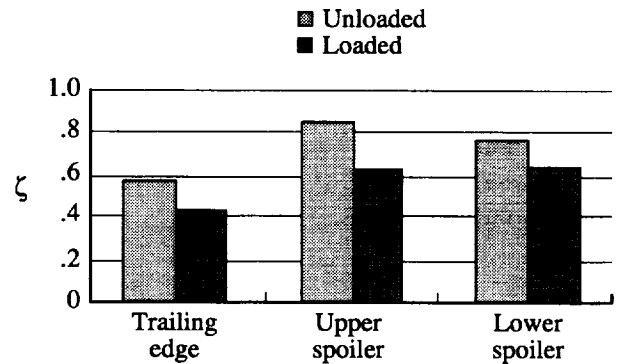Figure 11. Frequency parameter ω for unloaded and loaded conditions early in wind tunnel test.

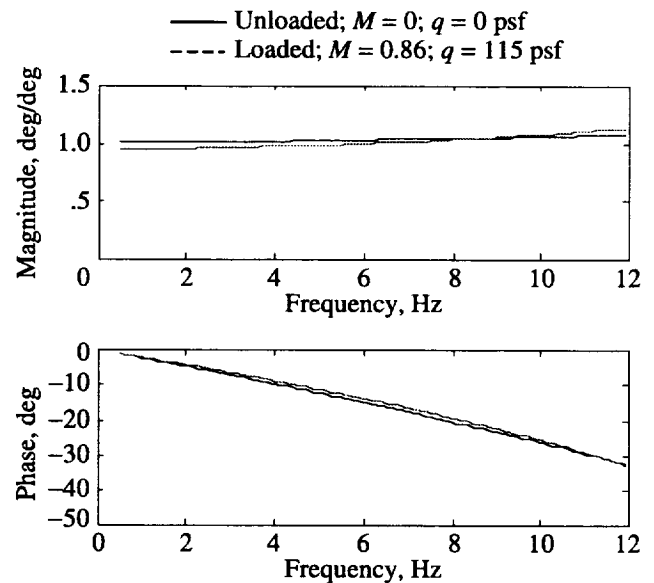Figure 12. Damping parameter ζ for unloaded and loaded conditions early in wind tunnel test.

Figure 13. Effect of aerodynamic load for trailing-edge actuator frequency response early in wind tunnel test.

Note that the loaded conditions correspond to different Mach numbers and dynamic pressures and thus characterize the qualitative effects of hinge load. Note also that the comparisons at the early stage of the test are effectively isolated from wear and gain variations because little wear and no gain changes had yet occurred; this is not true for the middle and late stages of the test. Therefore, comparisons between the loaded and unloaded parameter estimates at the middle and late stages combine all the possible effects.

Despite these differences, the influence of aerodynamic loading had no significant impact on any of the actuator frequency responses in the frequency range of interest (0.5 to 12 hertz), as shown in figure 13. Additional plots are presented in the appendix that show the effects of aerodynamic loading.

The actuator frequency responses, as a whole, varied little over time and under aerodynamic load throughout the wind tunnel test. This lack of variation would imply that very simple actuator models could be used in the analysis, design, and simulation of control systems for the BACT wind tunnel model. The actuators can be effectively modeled by constant coefficient, second-order transfer functions of the form shown in equation (6). The coefficients do not, in general, have to be scheduled with hinge load but some scheduling for wear state might be required if small phase variations are an issue in control system design. In addition, the parameter variations presented in tables 1 and 2 could be used to quantify typical

10

actuator uncertainties for application to robustness studies of BACT controllers.

Concluding Remarks

Experimental actuator frequency response data, generated during an experiment involving the Benchmark Active Control Technology (BACT) wind tunnel model in the Langley Transonic Dynamics Tunnel, were used as a basis for estimation of parameters in transfer function models of the BACT actuators. A parameter estimation approach based on minimizing the difference between experimental and model-based frequency responses was successfully employed to model the dynamic characteristics of the actuators of the BACT wind tunnel model using third-order, constant coefficient transfer functions. It was also determined that the actuator model could be reduced to second order with negligible impact on the frequency response properties over the frequency range for which experimental data were available.

Model-based frequency response data closely approximated the experimental data over a wide range of wind tunnel operating conditions. Comparative analysis of the analytical data corresponding to various test conditions also indicated little change in actuator frequency response behavior due to mechanical wear, servo gain variations, and aerodynamic load. As a result, the transfer function models developed herein can be used to model the dynamics of the BACT actuators over a wide range of wind tunnel operating conditions for application to control system design and analysis. In addition, the parameter variations associated with mechanical wear, servo gain variations, and aerodynamic loading effects can be used to develop uncertainty models of the actuators for application to robustness analysis of BACT controllers.

NASA Langley Research Center
Hampton, VA 23681-2199
May 15, 1998

References

1. Durham, Michael H.; Keller, Donald F.; Bennett, Robert M.; and Wieseman, Carol D.: A Status Report on a Model for Benchmark Active Controls Testing. AIAA-91-1011, Apr. 1991.

2. Waszak, Martin R.: Modeling the Benchmark Active Control Technology Wind-Tunnel Model for Application to Flutter Suppression. AIAA-96-3437, July 1996.

3. Hardin, J. C.: *Introduction to Time Series Analysis.* NASA RP-1145, 1986.

4. Bennett, Robert M.; Eckstrom, Clinton V.; Rivera, Jose A., Jr.; Dansberry, Bryan E.; Farmer, Moses G.; and Durham, Michael H.: *The Benchmark Aeroelastic Models Program—Description and Highlights of Initial Results.* NASA TM-104180, 1991.

5. Rivera, Jose A., Jr.; Dansberry, Bryan E.; Bennett, Robert M.; Durham, Michael H.; and Silva, Walter A.: NACA 0012 Benchmark Model Experimental Flutter Results With Unsteady Pressure Distributions. *Thirty-Third AIAA/ASME/ASCE/AHS/ASC Structures, Structural Dynamics and Materials Conference—Technical Papers,* Part 4, 1992, pp. 1898–1908. (Available as AIAA-92-2396.)

6. Rivera, Jose A., Jr.; Dansberry, Bryan E.; Durham, Michael H.; Bennett, Robert M.; and Silva, Walter A.: *Pressure Measurements on a Rectangular Wing With a NACA 0012 Airfoil During Conventional Flutter.* NASA TM-104211, 1992.

7. Baals, D. D.; and Corliss, W. R.: *Wind Tunnels of NASA.* NASA SP-440, 1981.

8. Sorokach, Michael R., Jr.: Miniature Linear-to-Rotary Motion Actuator. *The 27th Aerospace Mechanisms Symposium,* Ron Mancini, ed., NASA CP-3205, 1993, pp. 299–314.

9. Wieseman, Carol D.; Hoadley, Sherwood T.; and McGraw, Sandra M.: On-Line Analysis Capabilities Developed To Support the Active Flexible Wing Wind-Tunnel Tests. *J. Aircr.,* vol. 32, no. 1, Jan.–Feb. 1995, pp. 39–44.

10. Truxal, John G.: *Control Engineers' Handbook—Servomechanisms, Regulators, and Automatic Feedback Control Systems.* McGraw-Hill Book Co., Inc., 1958.

11. Buttrill, Carey S.; Bacon, Barton J.; Heeg, Jennifer; Houck, Jacob A.; and Wood, David V.: *Aeroservoelastic Simulation of an Active Flexible Wing Wind Tunnel Model.* NASA TP-3510, 1996.

12. Gill, Philip E.; Murray, Walter; and Wright, Margaret H.: *Practical Optimization.* Academic Press, 1981.

13. Grace, Andrew: *Optimization Toolbox for Use With MATLAB®.* The MathWorks, Inc., 1994.

Appendix

Additional Frequency Response Plots

This appendix consists of additional actuator frequency response plots of both experimental and analytical data corresponding to different times (i.e., levels of wear) and loading conditions. All the plots are in a similar format. Each figure contains several plots, corresponding to frequency response magnitude and phase versus frequency of the control surface position with respect to control surface command for the trailing-edge flap TE, upper spoiler US, and lower spoiler LS actuators. Each plot is linearly scaled with magnitude values ranging between 0 and 1.5 deg/deg and phase values ranging between $-50°$ and $0°$. Frequency values range between 0.5 and 12 hertz. Aerodynamically unloaded cases correspond to zero Mach number M and dynamic pressure q conditions. Aerodynamically loaded cases correspond to a range of Mach numbers between 0.63 and 0.91 and dynamic pressures between 74 and 190 psf and thus represent only qualitative effects of hinge load. To establish a reference for chronological comparison, three data sets were chosen to represent data acquired near the beginning, near the middle, and near the end of the wind tunnel test and are referred to as "Early," "Middle," and "Late," respectively.

Figures A1 and A2 depict frequency response plots for experimental data over time with and without aerodynamic load. Figures A3 and A4 depict frequency response plots for the analytical data based on the actuator model in equation (1) with the parameters resulting from the parameter identification process with and without aerodynamic load. Figures A5, A6, and A7 depict frequency response plots for the experimental and analytical data with no aerodynamic hinge loading for the TE, US, and LS actuators, respectively. Figures A8 through A10 depict the corresponding frequency response plots for the actuators under load.
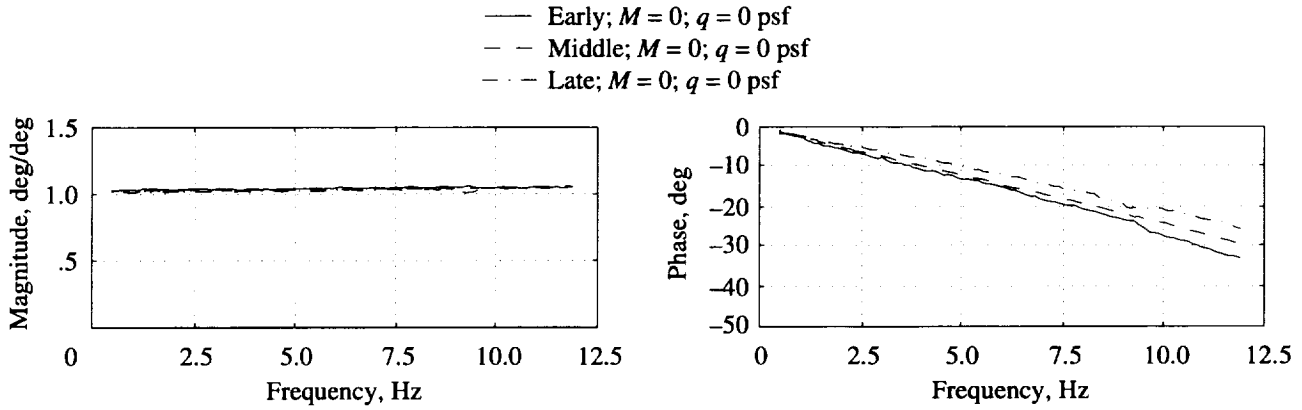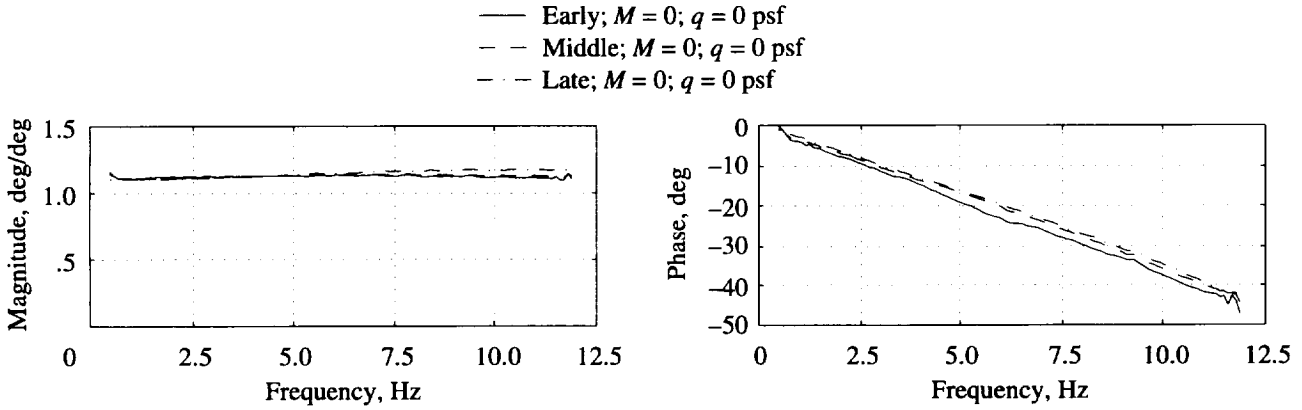
12

(a) Trailing-edge actuator frequency response.

(b) Upper spoiler actuator frequency response.
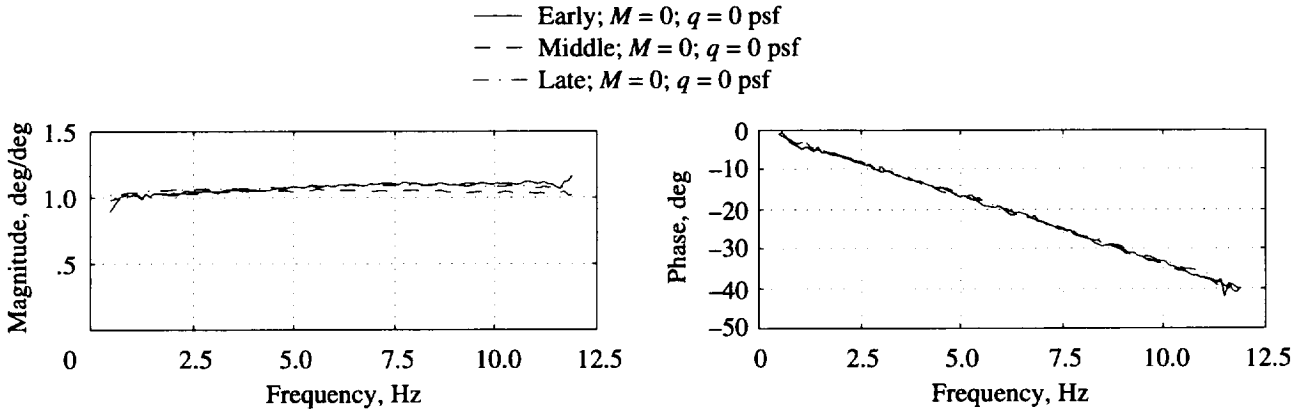
(c) Lower spoiler actuator frequency response.

Figure A1. Experimental actuator frequency response plots for no aerodynamic load (δ/δ_c).
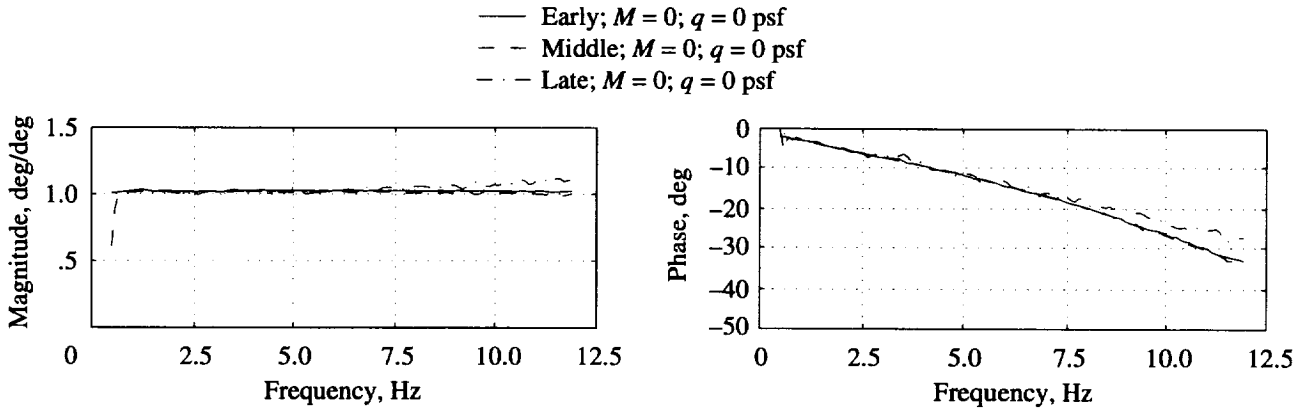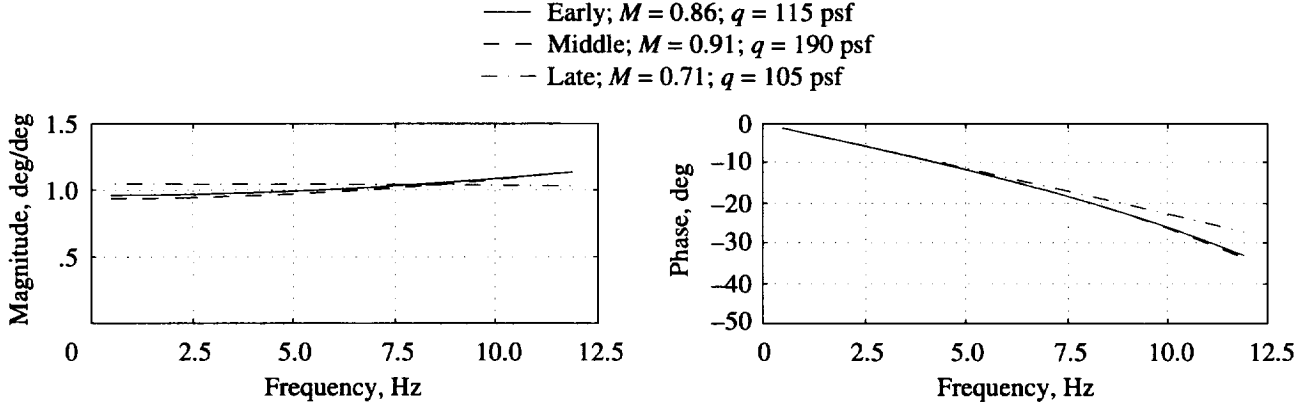
13

(a) Trailing-edge actuator frequency response.
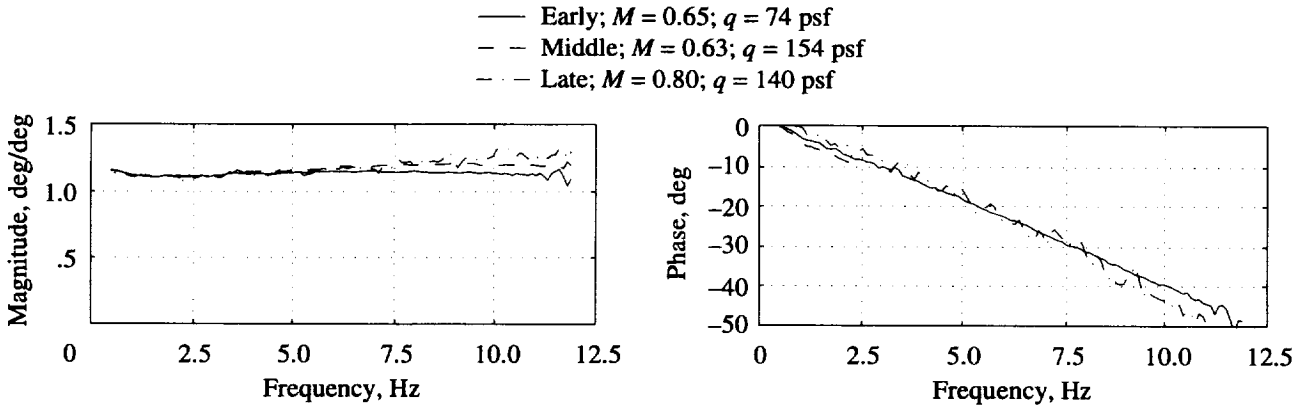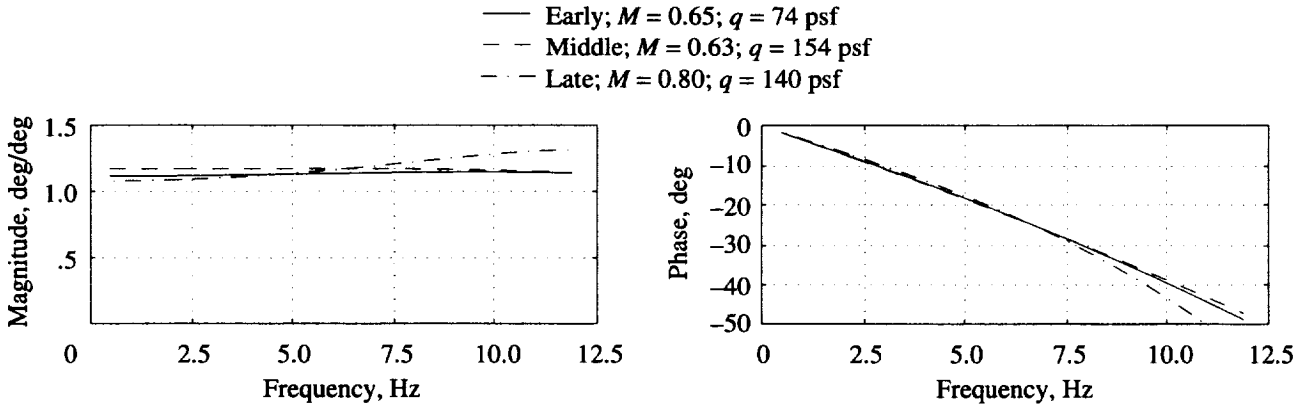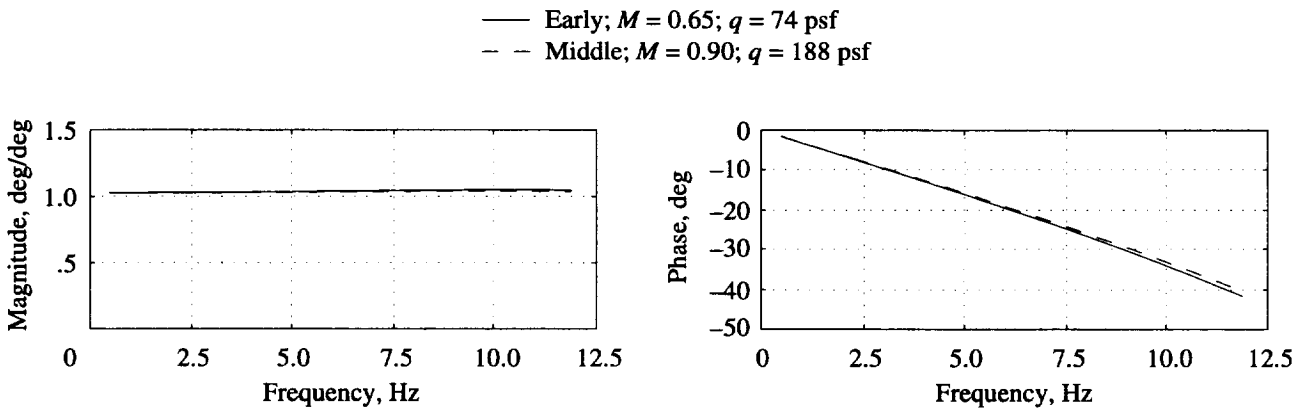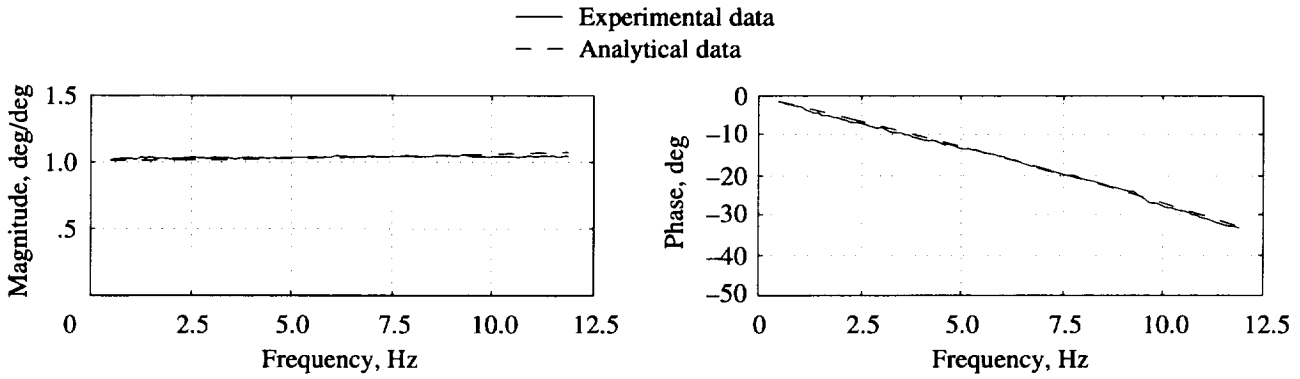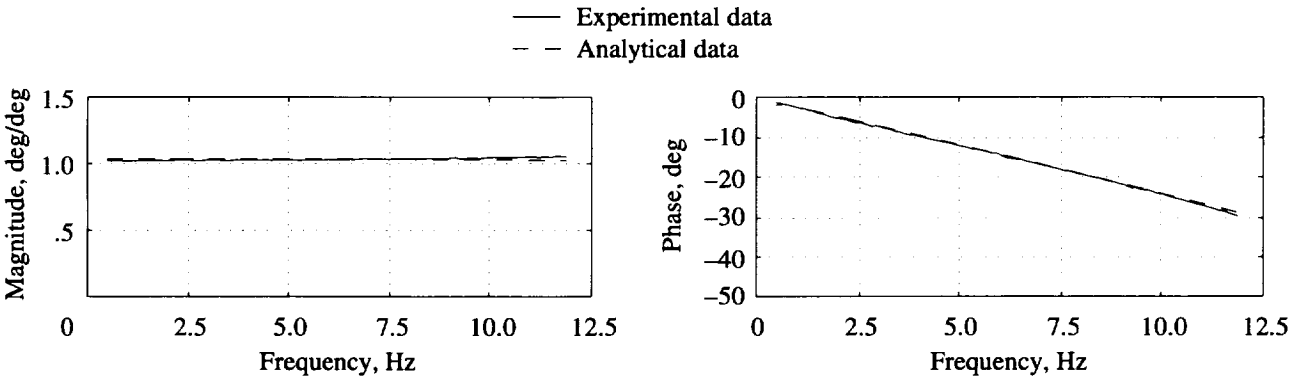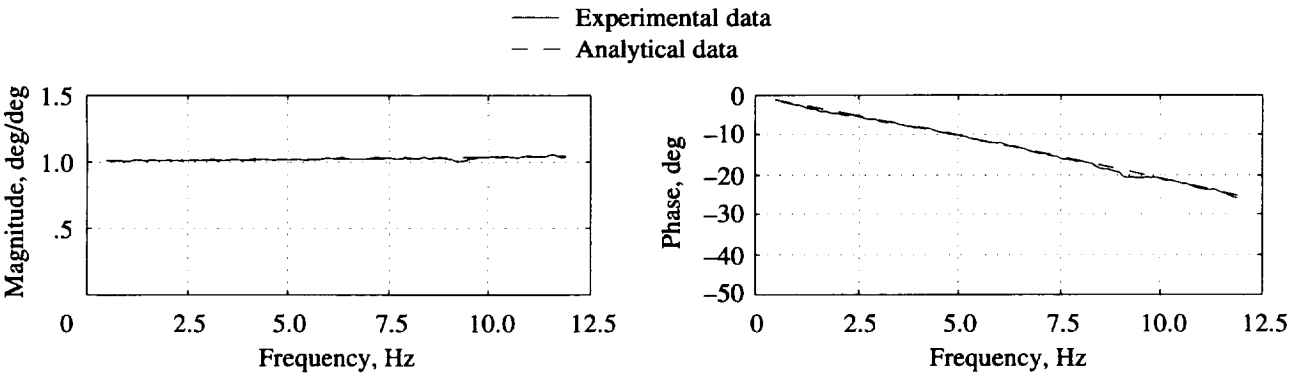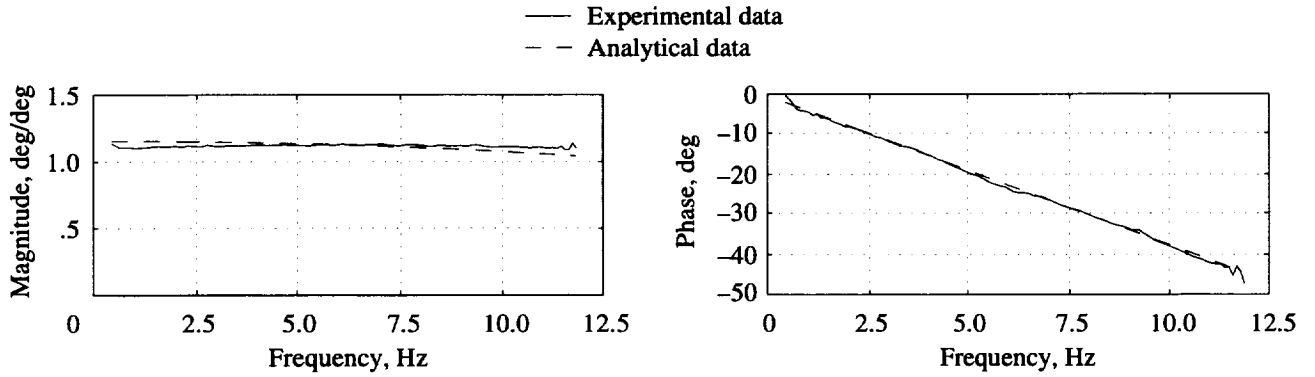

(b) Upper spoiler actuator frequency response.
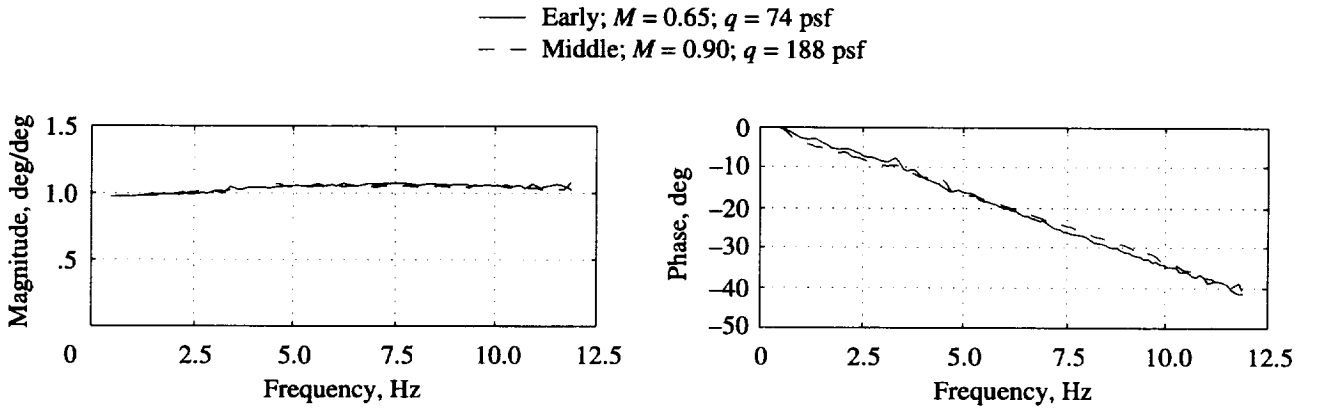
(c) Lower spoiler actuator frequency response.

Figure A2. Experimental actuator frequency response plots for aerodynamic load (δ/δ_c).
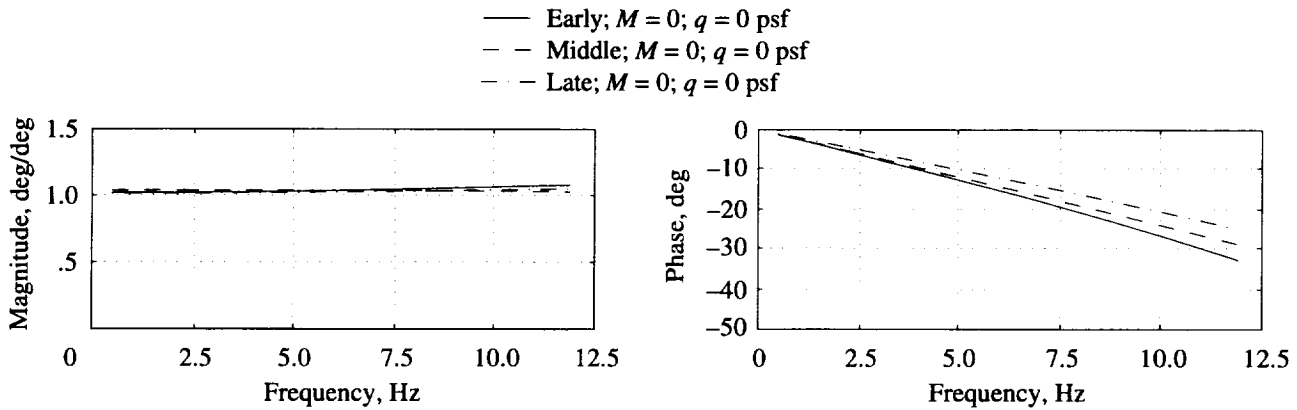
(a) Trailing-edge actuator frequency response.
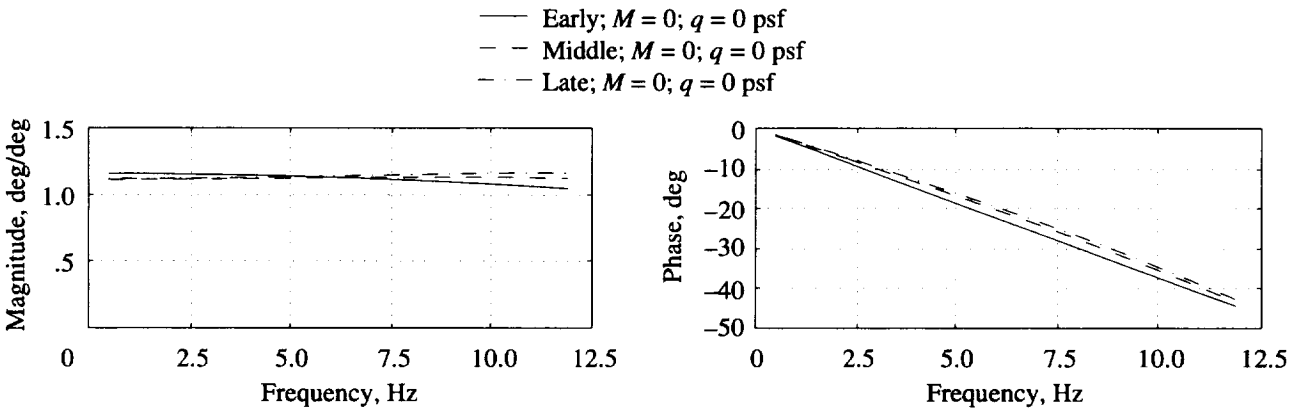
(b) Upper spoiler actuator frequency response.
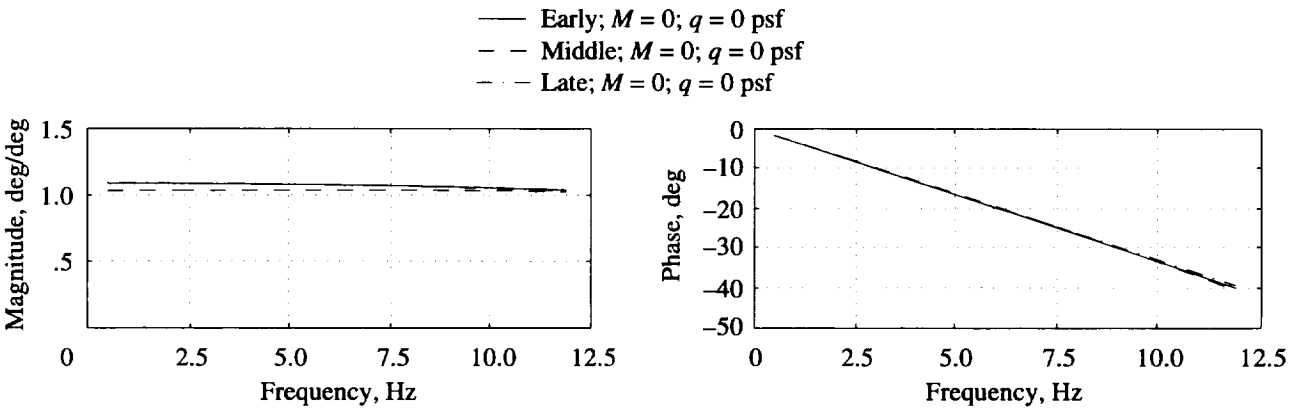
(c) Lower spoiler actuator frequency response.

Figure A3. Analytical actuator frequency response plots for no aerodynamic load (δ/δ_c).

(a) Trailing-edge actuator frequency response.

(b) Upper spoiler actuator frequency response.

(c) Lower spoiler actuator frequency response.

Figure A4. Analytical actuator frequency response plots for aerodynamic load (δ/δ_c).

(a) Trailing-edge actuator frequency response; early in test.

(b) Trailing-edge actuator frequency response; middle of test.

(c) Trailing-edge actuator frequency response; late in test.

Figure A5. Experimental and analytical trailing-edge actuator frequency responses for no aerodynamic load (δ/δ_c).

17

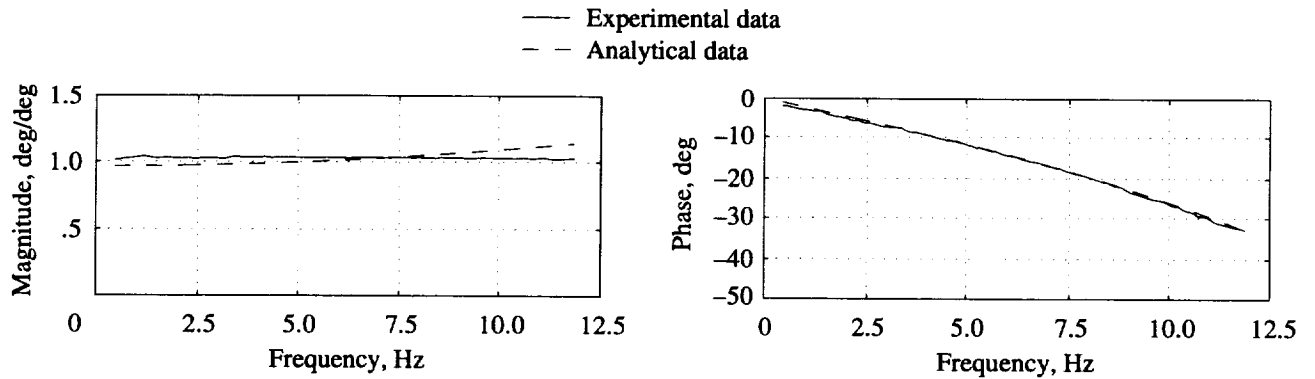(a) Upper spoiler frequency response; early in test.
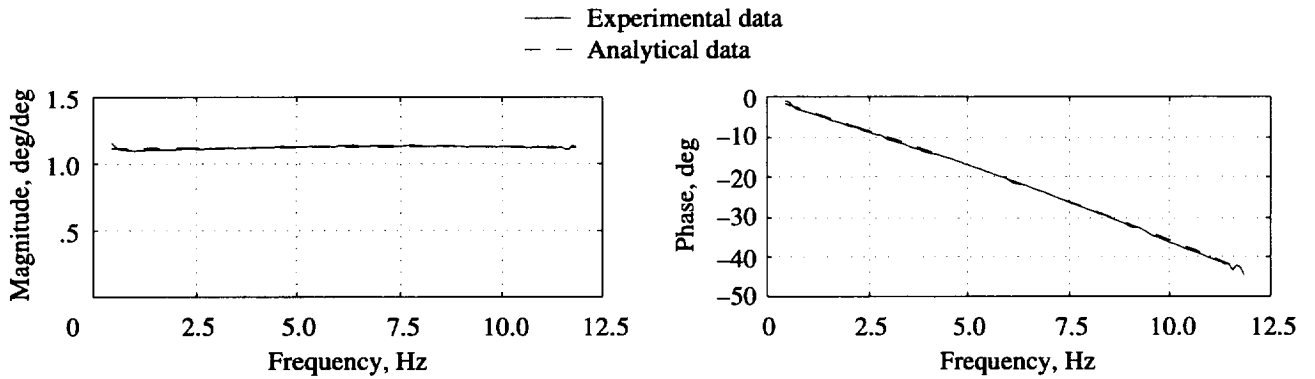
(b) Upper spoiler frequency response; middle of test.
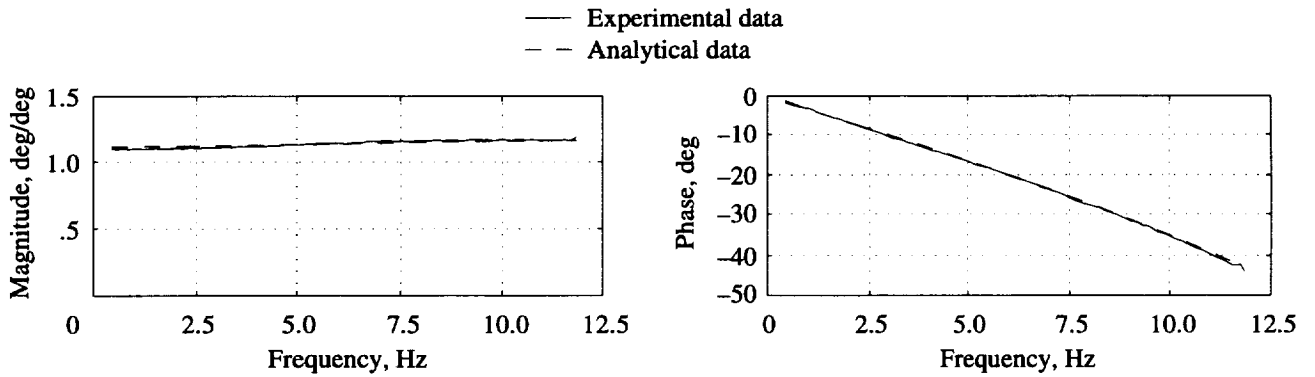
(c) Upper spoiler frequency response; late in test.

Figure A6. Experimental and analytical upper spoiler actuator frequency responses for no aerodynamic load (δ/δ_c).
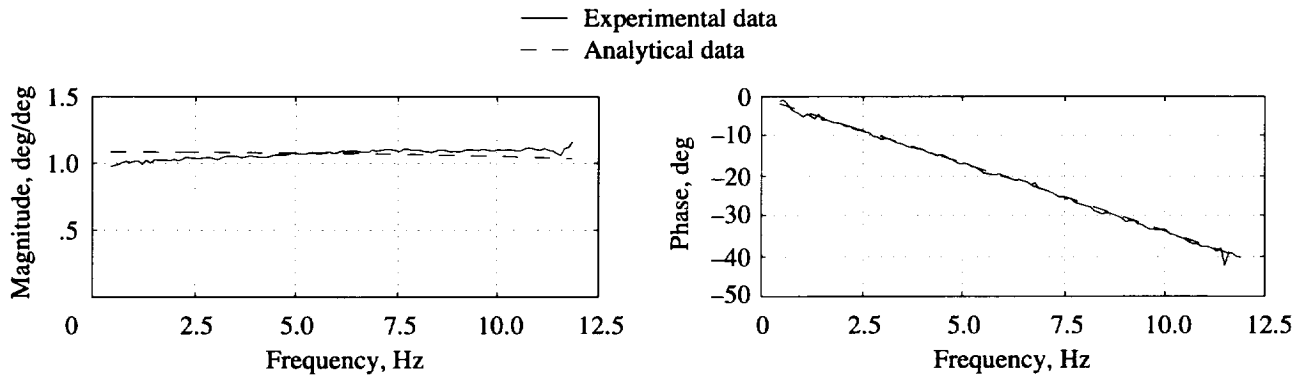
(a) Lower spoiler frequency response; early in test.
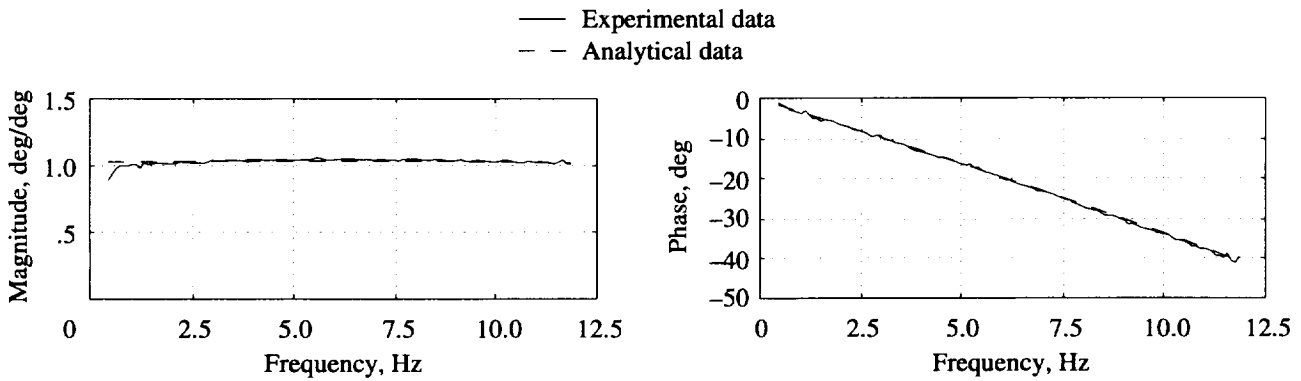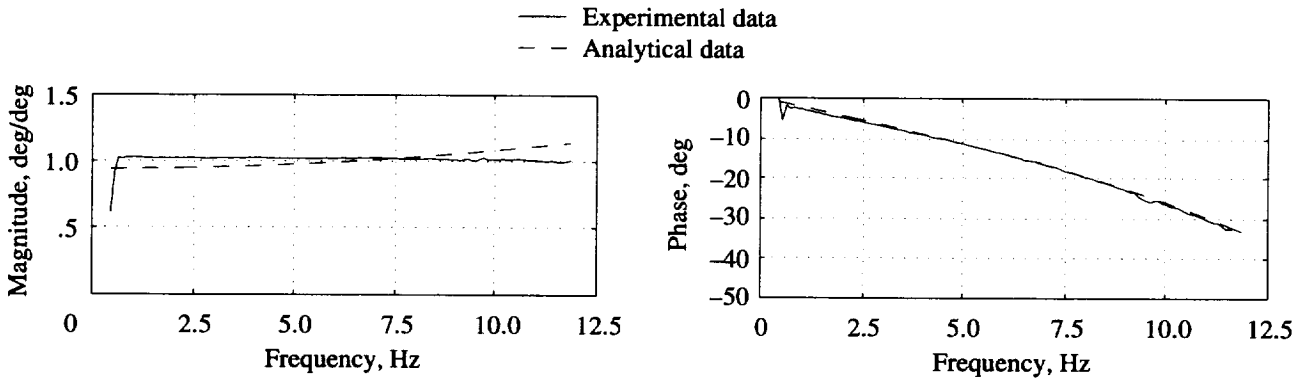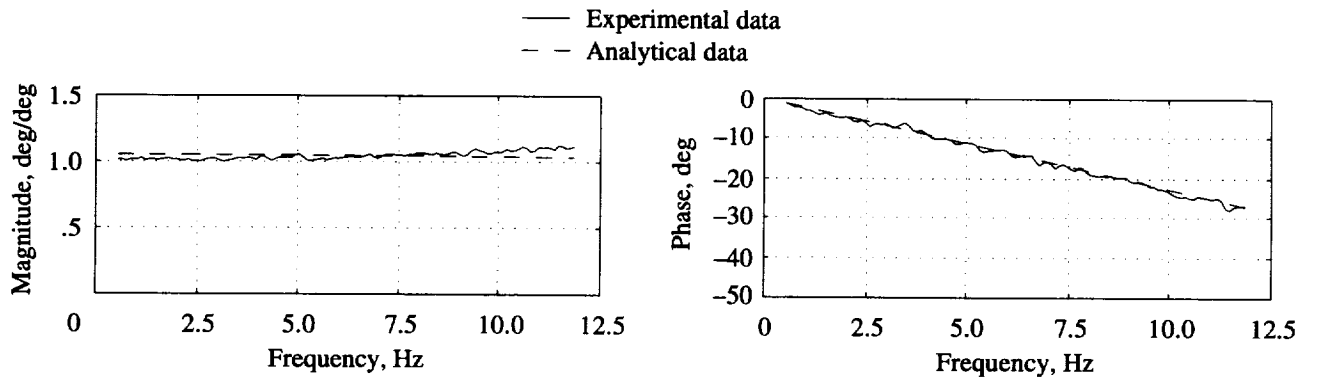

(b) Lower spoiler frequency response; middle of test.
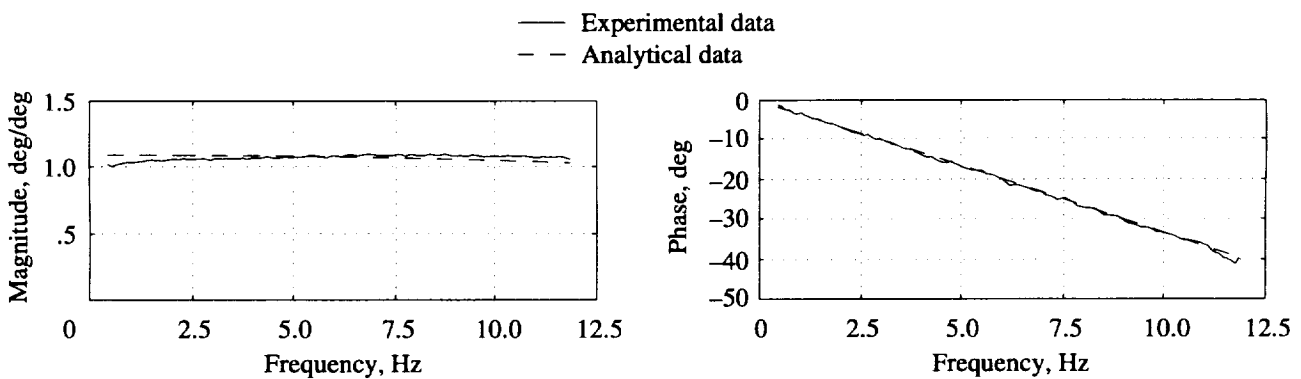
(c) Lower spoiler frequency response; late in test.

Figure A7. Experimental and analytical lower spoiler actuator frequency responses for no aerodynamic load (δ/δ_c).

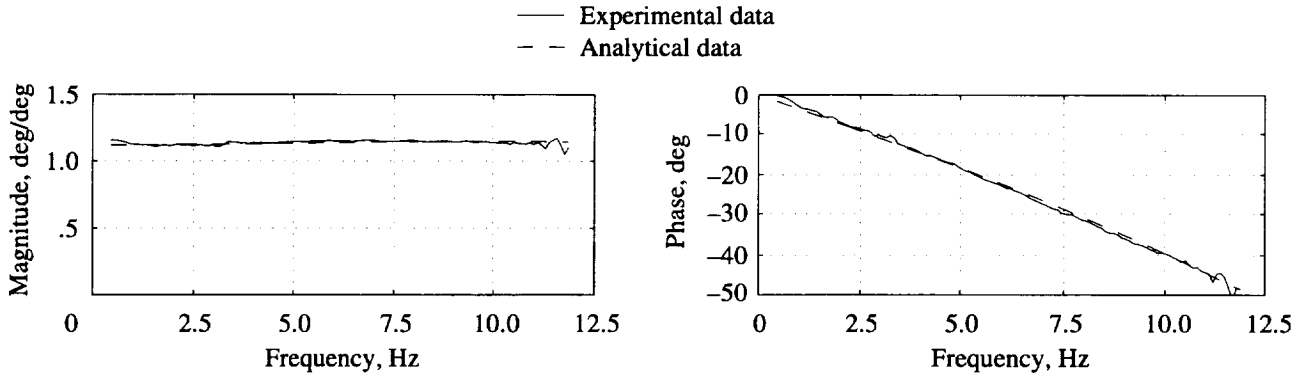(a) Trailing-edge actuator frequency response; early in test; $M = 0.86$; $q = 115$ psf.

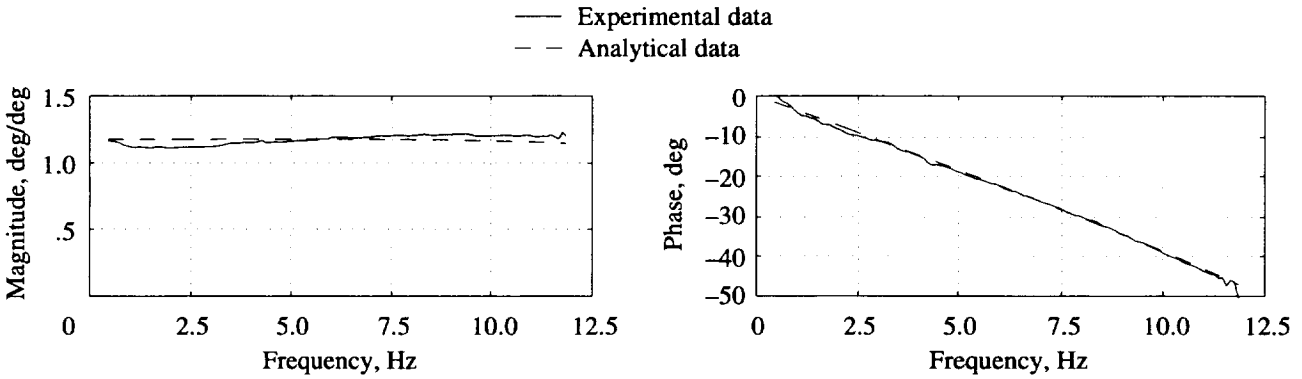(b) Trailing-edge actuator frequency response; middle of test; $M = 0.91$; $q = 190$ psf.

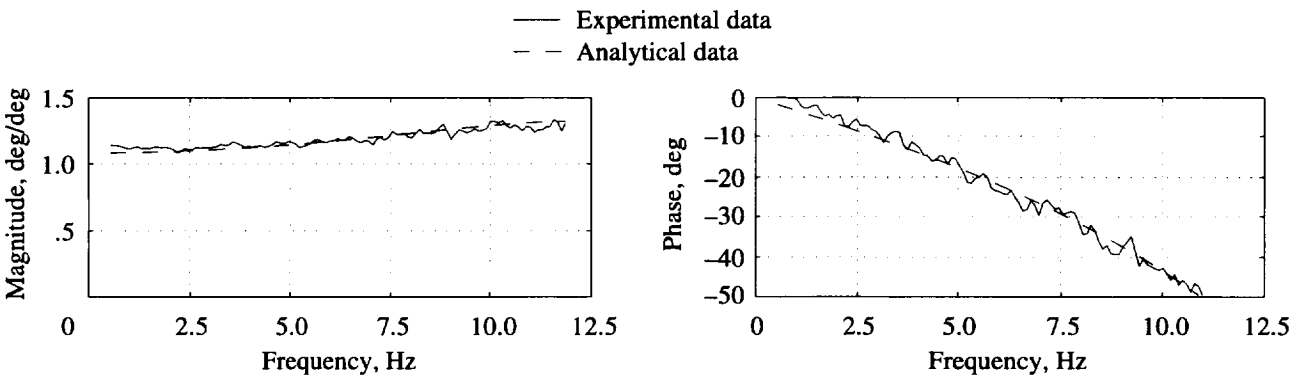(c) Trailing-edge actuator frequency response; late in test; $M = 0.71$; $q = 105$ psf.

Figure A8. Experimental and analytical trailing-edge actuator frequency responses for aerodynamic load (δ/δ_c).

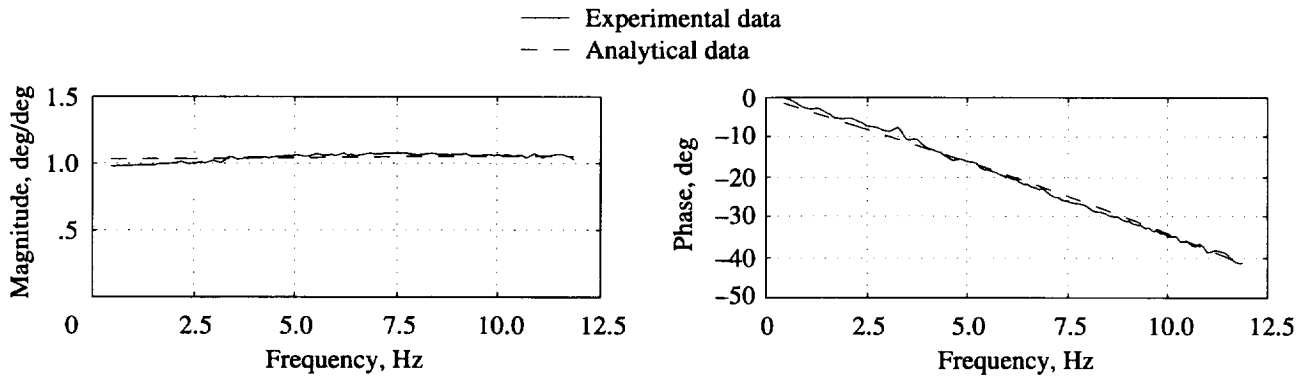(a) Upper spoiler frequency response; early in test; $M = 0.65$; $q = 74$ psf.

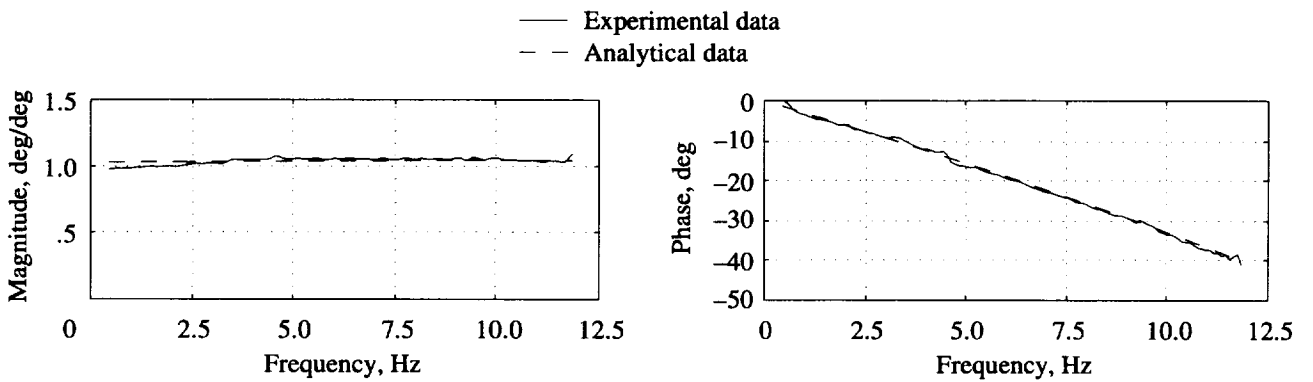(b) Upper spoiler frequency response; middle of test; $M = 0.63$; $q = 154$ psf.

(c) Upper spoiler frequency response; late in test; $M = 0.80$; $q = 140$ psf.

Figure A9. Experimental and analytical upper spoiler actuator frequency responses for aerodynamic load (δ/δ_c).

(a) Lower spoiler frequency response; early in test; $M = 0.65$; $q = 74$ psf.

(b) Lower spoiler frequency response; middle of test; $M = 0.90$; $q = 188$ psf.

Figure A10. Experimental and analytical lower spoiler actuator frequency responses for aerodynamic load (δ/δ_c).

REPORT DOCUMENTATION PAGE

1. AGENCY USE ONLY *(Leave blank)*	2. REPORT DATE	3. REPORT TYPE AND DATES COVERED
	July 1998	Technical Memorandum

4. TITLE AND SUBTITLE
Parameter Estimation of Actuators for Benchmark Active Control Technology (BACT) Wind Tunnel Model With Analysis of Wear and Aerodynamic Loading Effects

5. FUNDING NUMBERS
WU 505-64-52-01

6. AUTHOR(S)
Martin R. Waszak and Jimmy Fung

7. PERFORMING ORGANIZATION NAME(S) AND ADDRESS(ES)
NASA Langley Research Center
Hampton, VA 23681-2199

8. PERFORMING ORGANIZATION REPORT NUMBER
L-17540

9. SPONSORING/MONITORING AGENCY NAME(S) AND ADDRESS(ES)
National Aeronautics and Space Administration
Washington, DC 20546-0001

10. SPONSORING/MONITORING AGENCY REPORT NUMBER
NASA/TM-1998-208452

11. SUPPLEMENTARY NOTES
Part of the information presented in this report was included in a paper (AIAA-96-3362) presented at the AIAA Atmospheric Flight Mechanics Conference, San Diego, CA, July 29–31, 1996.

12a. DISTRIBUTION/AVAILABILITY STATEMENT
Unclassified–Unlimited
Subject Category 08   Distribution: Standard
Availability: NASA CASI (301) 621-0390

12b. DISTRIBUTION CODE

13. ABSTRACT *(Maximum 200 words)*
This report describes the development of transfer function models for the trailing-edge and upper and lower spoiler actuators of the Benchmark Active Control Technology (BACT) wind tunnel model for application to control system analysis and design. A simple nonlinear least-squares parameter estimation approach is applied to determine transfer function parameters from frequency response data. Unconstrained quasi-Newton minimization of weighted frequency response error was employed to estimate the transfer function parameters. An analysis of the behavior of the actuators over time to assess the effects of wear and aerodynamic load by using the transfer function models is also presented. The frequency responses indicate consistent actuator behavior throughout the wind tunnel test and only slight degradation in effectiveness due to aerodynamic hinge loading. The resulting actuator models have been used in design, analysis, and simulation of controllers for the BACT to successfully suppress flutter over a wide range of conditions.

14. SUBJECT TERMS
Actuator dynamics; Parameter estimation; Optimization

15. NUMBER OF PAGES
31

16. PRICE CODE
A03

17. SECURITY CLASSIFICATION OF REPORT	18. SECURITY CLASSIFICATION OF THIS PAGE	19. SECURITY CLASSIFICATION OF ABSTRACT	20. LIMITATION OF ABSTRACT
Unclassified	Unclassified	Unclassified	